Letters

Negative-Sequence Current Compensation Using a PI+Resonant Controller in a Single Synchronous Reference Frame

Suman Ghosh, *Graduate Student Member, IEEE*, and Kenichiro Sano, *Senior Member, IEEE*

***Abstract*—Conventional current control methods for grid-connected inverters often face challenges under unbalanced grid conditions and frequency variations. Although proportional–integral (PI) controllers in the synchronous reference (dq) frame perform well for positive-sequence regulation, they require dual dq frames to handle negative-sequence components, increasing computational complexity. Proportional–resonant (PR) controllers in the stationary ($\alpha\beta$) frame offer direct ac tracking but suffer from degraded performance under grid frequency deviations, limiting compliance with grid codes. To address these limitations, this letter proposes a novel PI + resonant controller operating entirely in the positive-sequence dq frame. It combines a conventional PI controller for positive-sequence current regulation with a resonant term tuned to twice the grid frequency to regulate negative-sequence currents. This single-frame implementation reduces computational burden by almost 25% compared to the method with dual dq frames while maintaining robustness under unbalanced grid conditions and frequency variation. The simulation results demonstrate the effectiveness of the proposed method compared to conventional PI and PR control strategies.**

***Index Terms*—Current control, grid-connected inverter, negative-sequence compensation, proportional–integral (PI) controller, resonant controller.**

I. Introduction

CURRENT control strategies for grid-connected inverters are typically implemented either in the synchronous reference (dq) frame or in the stationary ($\alpha\beta$) frame. Each approach offers distinct advantages but also faces challenges, especially when dealing with unbalanced grid conditions and frequency variations. Various control strategies for grid-connected converters are comprehensively reviewed in [1]. Among these, one of the most widely adopted approaches is active and reactive power control using the synchronous reference frame (SRF) transformation [2]. In this method, the Park transformation converts three-phase voltage and current signals into a positive-sequence dq frame, where the positive-sequence components appear as constant (dc) values. This simplifies the control problem since the proportional–integral (PI) controller can regulate these dc quantities efficiently, achieving fast dynamic response and zero steady-state error under balanced grid conditions. However, under grid unbalance or unbalanced load conditions, negative-sequence components arise. In the positive-sequence dq frame, these appear as oscillations at twice the grid frequency (2ω), which cannot be compensated by a PI controller alone. These oscillations deteriorate current tracking accuracy and increase harmonic distortion, thus degrading power quality.

To address this issue, the double synchronous reference frame (DSRF) method has been widely used [3]. DSRF employs two separate dq frames: one aligned with the positive-sequence components and the other with the negative-sequence components. This allows for independent and accurate control of both sequences. However, the interaction between positive and negative sequences gives rise to a coupled second harmonic component in each d-axis or q-axis. As a result, positive- and negative-sequence currents cannot be controlled independently. To achieve decoupled control of dual sequences, common sequence separation methods include notch filters and dual second order generalized integrators. In [4], a scheme based on the decoupled double SRF (DDSRF) is used to suppress the coupled second harmonic component. However, it requires additional low-pass digital filters (LPF) with relatively low cutoff frequency. While effective, DDSRF increases computational load due to additional coordinate transformations and filtering stages, requiring a higher processing capability from the controller. In [5], a self-decoupled dual sequence current control (SDDSCC) is proposed. The SDDSCC achieves decoupling of the positive- and negative-sequence currents in the double SRF without using a sequence extractor or any specialized dq decoupling method. However, the SDDSCC does not achieve complete dq decoupling due to the absence of the cross-coupling ωL terms in the control loops.

Alternatively, active/reactive power control can also be implemented with controllers based on the stationary ($\alpha\beta$) frame, eliminating the need for complex transformations. The proportional–resonant (PR) controller [6] can directly regulate sinusoidal current without coordinate transformation with zero steady-state error by incorporating a resonant term tuned to the fundamental frequency of the grid voltage. The PR controller effectively regulates ac currents, making it suitable for

Received 12 September 2025; revised 13 November 2025 and 10 December 2025; accepted 18 December 2025. Date of publication 23 December 2025; date of current version 19 January 2026. *(Corresponding author: Suman Ghosh.)*

The authors are with the Department of Electrical and Electronic Engineering, Institute of Science Tokyo, Tokyo 152-8552, Japan (e-mail: ghosh.s@pel.ee.eng.isct.ac.jp; sano@ee.eng.isct.ac.jp).

Color versions of one or more figures in this article are available at https://doi.org/10.1109/TPEL.2025.3647664.

Digital Object Identifier 10.1109/TPEL.2025.3647664

grid-connected inverter applications, especially under unbalanced conditions. In [7] and [8], the relationship between the PR controller in the $\alpha\beta$ frame and the PI controller in the dq frame is derived. The PI controller in dq frame is equivalent to the PR controller in $\alpha\beta$ frame for the fundamental frequency. However, PR controllers face significant challenges when the grid frequency varies. When the grid frequency drifts (e.g., from 50 to 48.5 Hz or 51.5 Hz), the resonant peak no longer aligns with the actual frequency, leading to residual steady-state error and degraded harmonic rejection. Since the resonant frequency is fixed, any deviation in grid frequency leads to a mismatch, causing degraded harmonic compensation and reduced current tracking performance. Hence, in applications where the grid frequency is not constant, PR-based control suffers performance degradation. Adaptive PR controllers, using a frequency-locked loops [9], have been proposed to address this issue. They offer improved current regulation characteristics compared to nonadaptive controllers. However, the resonant controller gains are usually fixed. These factors can affect the response of the compensating current injection. Santiprapan et al. [10] presented the adaptive PR controller using the fuzzy logic algorithm (FLA), in which the FLA is designed to adapt the suitable gain of the PR controller. The appropriate output gain of the PR controller can provide good performance for harmonic mitigation without redesign or adding the resonant terms. However, they increase complexity, and under unbalanced conditions, negative-sequence components cause additional control difficulties, as the $\alpha\beta$ frame does not decouple positive- and negative-sequence currents. Also, in the $\alpha\beta$ frame, positive-, negative-, and harmonic-sequence components coexist, with the positive sequence appearing at $+\omega_0$ and the negative sequence at $-\omega_0$. Because these components overlap in frequency, the controller cannot inherently distinguish between them. Therefore, separate control requires either multiple resonant terms at $\pm\omega_0$ or explicit sequence extraction, both of which introduce delay and computational load. Moreover, the α- and β-axes are dynamically coupled, and this coupling becomes more significant under unbalanced or distorted conditions, requiring additional decoupling networks that further increase computational effort.

Active disturbance rejection control (ADRC) with extended state observer (ESO) based control methods [12] can effectively estimate and compensate for unmodeled dynamics, harmonics, and parameter variations and offer robust performance for systems with complex and broadband disturbances. For grid-connected inverters under voltage unbalances or negative sequence compensation, however, the dominant disturbance is a well-characterized 2ω negative-sequence component. In this context, the full complexity of ADRC/ESO is not strictly necessary.

To overcome the limitations of both DDSRF and PR-based methods, this letter proposes a novel controller called the positive-frame-based PI + resonant (PIR) controller. The proposed PIR controller operates entirely within the positive-sequence dq frame. It enhances the conventional PI controller with a resonant term tuned to twice the grid frequency, enabling effective regulation of negative-sequence currents. This approach enables accurate control of both positive- and negative-sequence components using a single reference frame, significantly simplifying implementation. Moreover, the PIR controller is robust against grid frequency variations. Finally, the validity of the model is evaluated by simulations.

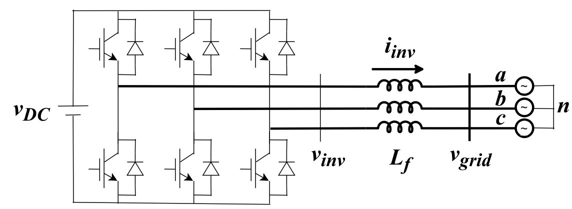

Fig. 1. System configuration.

TABLE I
CIRCUIT PARAMETERS

Grid voltage	V_{grid}	400 V
Grid frequency	f_{grid}	50 Hz
Filter inductance	L_f	1.5 mH
DC link voltage	v_{DC}	800 V
Proportional gain	k_p	5
Integral gain	k_i	400
Resonant gain	k_r	1000

II. SYSTEM CONFIGURATION

Fig. 1 illustrates the system configuration focused in this letter. It consists of a grid-connected inverter, filter inductors L_f, and a three-phase voltage source v_{grid} $(V_{\text{grid}}, f_{\text{grid}})$ imitating the utility grid. The circuit parameters are given in Table I.

An example application of the grid-connected inverter is in power quality conditioning systems with battery energy storage. The inverter must accurately control not only the positive-sequence current but also the negative-sequence current. It also needs to maintain stable positive-sequence current regulation under grid frequency variations.

III. PROPOSED CONTROL METHOD

Fig. 2 shows the proposed positive-frame-based PIR controller. The PIR controller operates entirely within a single positive-sequence dq frame, avoiding the complexity of dual-frame approaches, such as DDSRF. The measured grid voltages v_{grid} and inverter currents i_{inv} are transformed into the positive-sequence dq frame using the phase angle obtained from a single phase-locked loop (PLL). The control error between the reference currents i_d^* and i_q^*, and actual inverter currents i_d and i_q is processed through the PIR controller. To enhance transient performance and achieve decoupling, standard feedforward voltage compensation and cross-coupling terms ($\omega L I_q$ and $\omega L I_d$) are incorporated into the control loop. Grid voltage after dq transformation (v_d, v_q) are used as feedforward voltages instead of its positive-sequence components (v_d^+, v_q^+) to avoid additional filtering complexity. This is also because the resonant controller is specifically tuned to reject disturbances at 100 Hz. The resulting dq voltage commands v_d^* and v_q^* are then converted into three-phase voltage references v_{inv}^*, and passed to a pulsewidth modulation pulse generator.

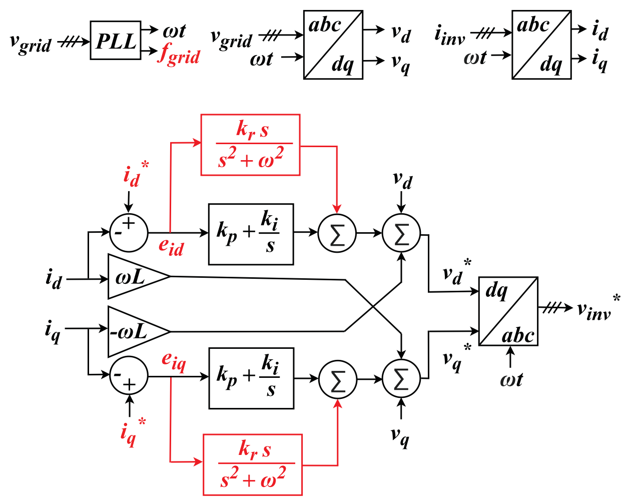

Fig. 2. Proposed current control based on the PIR controller in a single synchronous frame.

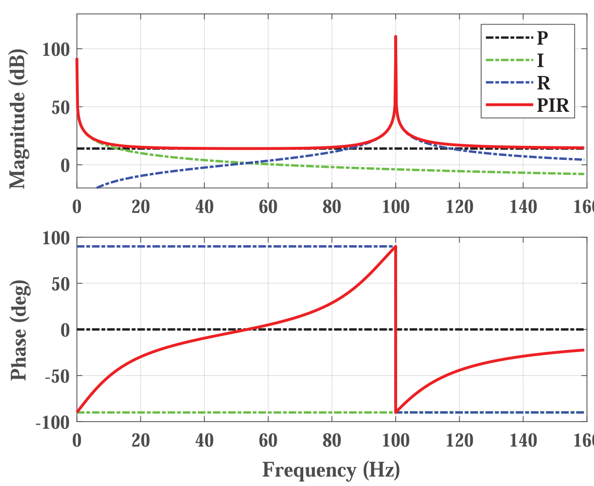

Fig. 3. Bode plot of PIR controller.

The proposed PIR controller consists of two parts: a conventional PI controller that regulates the positive-sequence currents (shown in black in Fig. 2), and a resonant controller that regulates the negative-sequence currents (shown in red in the figure). In the positive-sequence dq frame, the positive-sequence components appear as constant (dc) signals, which the PI controller can regulate effectively due to its infinite dc gain. In contrast, negative-sequence components are transformed into 100 Hz, which corresponds to twice the grid frequency, in the same dq frame, and cannot be sufficiently suppressed by the PI controller alone. To address this, a resonant controller tuned to 100 Hz is integrated into the dq-frame control loop. The resonant controller effectively regulates the negative-sequence currents. This eliminates the need for a separate negative-sequence reference frame, reducing computational burden and simplifying implementation. Fig. 3 shows the bode plot of the PIR controller. It can been clearly seen that the PIR controller has a very high gain at dc (0 Hz) and 100 Hz in the positive sequence dq frame. Thus, it can effectively compensate for both positive- and negative-sequence signals. Although transfer function of

TABLE II
COMPARISON OF CURRENT CONTROL STRATEGIES

Feature	DDSRF	PR	Proposed PIR
Frame Used	Dual dq	$\alpha\beta$	Single dq
Number of Clark Transformations	0	3	0
Number of Park Transformations	6	0	3
Current Control Loop	4 PI	2 PR	2 PIR
Number of additional LPF	4	0	0
Complexity	High	Low	Low
Freq. Robustness	High	Low	Moderate

the resonant term mathematically resembles an integrator at low frequency, it has negligible magnitude at dc, as clearly seen in R-plot in Fig. 3. At dc ($s = 0$) in the dq frame, the resonant term $G_{\mathrm{res}}(s)$ is equal to zero as follows:

$$G_{\mathrm{res}}(s) = \frac{k_r s}{s^2 + (2\omega)^2}, \quad G_{\mathrm{res}}(0) = 0.$$

Consequently, the additional resonant branch does not influence the positive-sequence control dynamics or reduce the stability margin.

Moreover, the controller retains the inherent robustness in regulating positive-sequence currents under grid frequency variations. As the PLL continuously tracks frequency changes, the fundamental frequency components remain as dc signals in the dq frame. Consequently, the control performance for positive-sequence currents does not deteriorate. This capability is essential for enabling the inverter to control active power in response to grid frequency variations.

Table II summarizes the comparison between different current control strategies in terms of the number of transformations, resonant terms, filters, etc. The DDSRF controller offers high-frequency robustness through dual dq frames but introduces complexity due to multiple frame transformations and decoupling terms. The PR controller, implemented in the stationary $\alpha\beta$ frame, is simpler but suffers from degraded performance under frequency deviations. The proposed PIR controller achieves a balance between these approaches by operating in a single positive-sequence dq frame, combining integral and resonant actions. It maintains low complexity, ensures accurate compensation under unbalanced conditions, and offers improved frequency robustness compared to PR, although slightly inferior to DDSRF.

IV. SIMULATION RESULTS AND DISCUSSION

To validate the proposed control strategy, simulations are conducted to demonstrate the controller's performance in a range of practical scenarios. First, selective positive-sequence and selective negative-sequence compensations are verified separately. Next, simultaneous compensation of both positive- and negative-sequence components is confirmed. Finally, the controller's robustness is evaluated under grid frequency variation (e.g., 48.5 Hz), confirming that the proposed method maintains

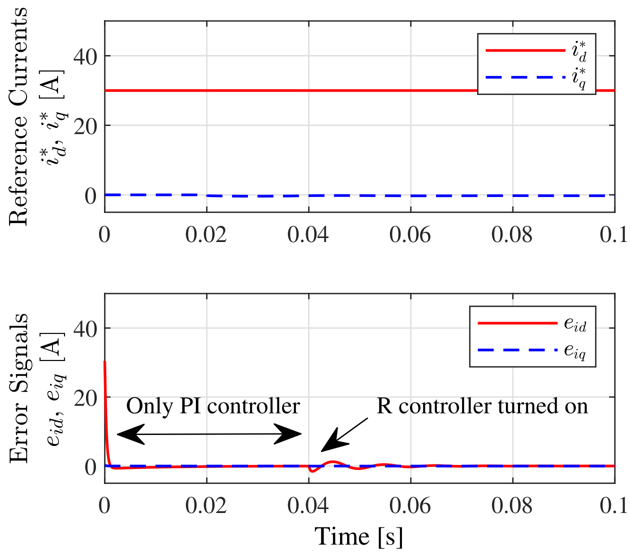

Fig. 4. Scenario 1: Positive-sequence compensation.

effective current regulation without the need for retuning or additional synchronization mechanisms.

A. Scenario 1: Only Positive-Sequence Compensation

Fig. 4 shows the simulation result for the case of positive-sequence compensation only. A reference value of 30 A is set for the positive-sequence current. The reference currents $i_d^* = 30$ A (dc) and $i_q^* = 0$ A (dc) represent a pure positive-sequence component. The error signals e_{id} and e_{iq} are also plotted.

Initially, from $t = 0$ to 0.04 s, the inverter operates with only the conventional PI controller. PI controllers can effectively regulate these dc quantities, as a result, e_{id} and e_{iq} are reduced to zero. At $t = 0.04$ s, the resonant part of the PIR controller is activated. However, the resonant part has no effect on the positive-sequence control performance and e_{id} and e_{iq} remain at zero.

B. Scenario 2: Only Negative-Sequence Compensation

Fig. 5 shows the simulation result for the case of negative-sequence compensation only. A reference value of 50 A is set for the negative-sequence current. The reference currents i_d^* and i_q^* represent a pure negative-sequence component. The error signals e_{id} and e_{iq} are plotted to demonstrate the effectiveness of the controller in minimizing tracking error.

Initially, from $t = 0$ to 0.04 s, the inverter operates with only the conventional PI controller. Due to the presence of 100 Hz oscillations in the synchronous dq frame, the PI controller alone is unable to fully track the oscillatory components in the reference current, resulting in 100 Hz error components in e_{id} and e_{iq}.

At $t = 0.04$ s, the resonant part of the PIR controller is activated. A clear improvement is observed after this instant: both e_{id} and e_{iq} are reduced to zero. This validates the capability of the proposed PIR controller to selectively track negative-sequence currents using only a single SRF.

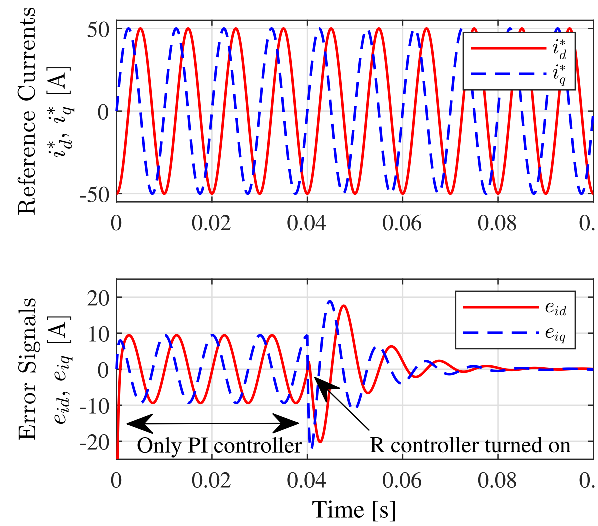

Fig. 5. Scenario 2: Negative-sequence compensation.

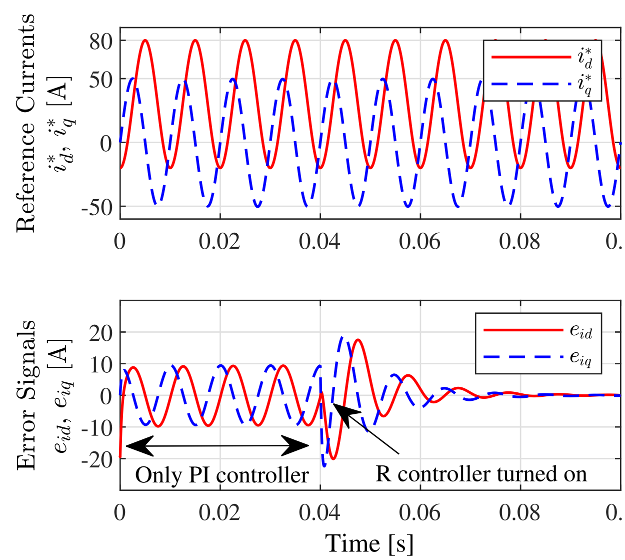

Fig. 6. Scenario 3: Simultaneous positive- and negative-sequence compensations.

C. Scenario 3: Simultaneous Positive- and Negative-Sequence Compensations

Fig. 6 shows the simulation result when the reference current includes both positive- and negative-sequence components. The positive- and negative-sequence reference currents are set to 30 A and 50 A, respectively. From $t = 0$ to 0.04 s, the inverter operates using only a PI controller. While the PI controller can regulate the dc (positive-sequence) component, it fails to fully track the oscillatory negative-sequence component. As a result, the mean value of e_{id} is zero, but still 100 Hz oscillations error component is present.

At $t = 0.04$ s, the resonant controller is activated, forming the complete PIR structure. Consequently, both e_{id} and e_{iq} are reduced to zero. This shows that the PIR controller can simultaneously regulate both sequences with high accuracy using a single dq frame.

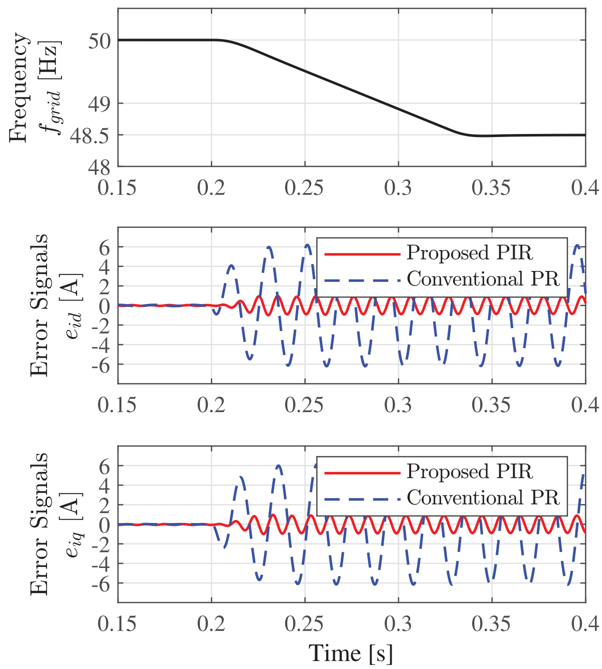

Fig. 7. Scenario 4: Robustness under grid frequency variation.

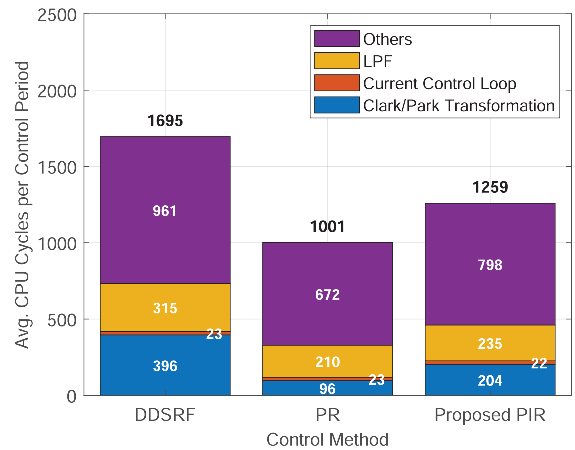

Fig. 8. Comparison of computational burden for different control methods.

D. Scenario 4: Robustness Under Grid Frequency Variation

Fig. 7 shows the simulation results under grid frequency variation. As per the Japanese grid-interconnection Code [11], the grid frequency permissible limit is ±1.5 Hz, beyond which underfrequency or overfrequency relays activate and trip the system. Therefore, in our studies, frequency deviations up to 48.5 Hz and 51.5 Hz have been considered, both yielding similar results. Hence, only the results for 48.5 Hz are presented here. The grid frequency is reduced to 48.5 Hz at $t = 0.2$ to 0.35 s to evaluate the controller's robustness. Simulations results are compared between the proposed PIR controller in the dq frame and the conventional PR controller in the $\alpha\beta$ frame. The resonant frequency is set to 100 Hz for the PIR controller and 50 Hz for the PR controller. The positive- and negative-sequence reference currents are set to 30 and 50 A, respectively.

Under frequency deviation, error signals e_{id} and e_{iq} increase in both controllers. The PR controller exhibits a noticeable steady-state error, whereas the PIR controller achieves superior compensation performance. The steady state error with conventional PR controller is very high at 6 A (peak) whereas with proposed PIR controller, its only 1 A (peak). No overshoot is observed. These results highlight the robustness of the PIR approach under grid frequency variations. If the resonant frequency of the resonant part was made adaptive, then the steady-state error could be eliminated entirely, which can be explored in future work.

V. Comparison of Computational Burden

The computational burden of different control methods was compared using a microcontroller (TI TMS320F28377S, 200 MHz Clock). DDSRF, PR, and proposed PIR controllers were coded in C and implemented on the microcontroller. Specifically, we measured the total computational cycles per control loop by accounting for all key operations, including Park/Clarke transformations, resonant terms, filters, and other arithmetic operations executed within one sampling period.

Fig. 8 summarizes the result. Comparing DDSRF and our proposed single frame PIR controller, single frame PIR controller achieves a reduction of approximately 25.72% in computational burden compared to the conventional DDSRF scheme, primarily due to the elimination of extra park transformations, lesser LPF, etc. In the calculation for $\alpha\beta$ frame PR controller, simple nonadaptive controller is modeled, and its computational burden is lower.

VI. Conclusion

This letter presented a novel current control strategy for grid-connected inverters using a positive-frame-based PIR controller operating entirely within a single synchronous reference (dq) frame. Unlike conventional DDSRF-based methods that require dual frames or PR controllers in the $\alpha\beta$ frame sensitive to frequency variations, the proposed approach achieves effective compensation of both positive-sequence and negative-sequence currents with significantly reduced control complexity. Simulation results in various scenarios, including selective positive-sequence, selective negative-sequence compensation, simultaneous positive- and negative-sequence controls, and operation at an off-nominal grid frequency (48.5 Hz)—demonstrated that the PIR controller maintains accurate and robust current regulation without retuning or additional synchronization mechanisms. The ability to suppress 100 Hz oscillations caused by negative-sequence components, combined with the inherent simplicity and robustness, makes the proposed method a practical and efficient solution for grid-connected inverters operating under three-phase unbalanced conditions. In this work, the focus was on proposing and validating the current controller through concept verification and dynamic response analysis using detailed simulations. Future work will involve hardware-in-the-loop and experimental validation to further confirm the controller's real-time performance and robustness under practical operating conditions.

REFERENCES

[1] R. Teodorescu, M. Liserre, and P. Rodrıǵuez, *Grid Converters for Photovoltaic and Wind Power Systems*. Chichester, U.K.: Wiley, 2011.

[2] M. P. Kazmierkowski and L. Malesani, "Current control techniques for three-phase voltage-source PWM converters: A survey," *IEEE Trans. Ind. Electron.*, vol. 45, no. 5, pp. 691–703, Oct. 1998.

[3] H. S. Song and K. Nam, "Dual current control scheme for PWM converter under unbalanced input voltage conditions," *IEEE Trans. Ind. Electron.*, vol. 46, no. 5, pp. 953–959, Oct. 1999.

[4] P. Rodriguez, J. Pou, J. Bergas, J. I. Candela, R. P. Burgos, and D. Boroyevich, "Decoupled double synchronous reference frame PLL for power converters control," *IEEE Trans. Power Electron.*, vol. 22, no. 2, pp. 584–592, Mar. 2007.

[5] X. Wang and L. Peng, "Self-decoupled dual sequence current control of D-STATCOM under unbalanced grid voltage," *IEEE Trans. Power Electron.*, vol. 39, no. 5, pp. 6191–6203, May 2024.

[6] Y. Sato, T. Ishizuka, K. Nezu, and T. Kataoka, "A new control strategy for voltage-type PWM rectifiers to realize zero steady-state control error in input current," *IEEE Trans. Ind. Appl.*, vol. 34, no. 3, pp. 480–486, May/Jun. 1998.

[7] C. Zou, B. Liu, S. Duan, and R. Li, "Stationary frame equivalent model of proportional-integral controller in dq synchronous frame," *IEEE Trans. Power Electron.*, vol. 29, no. 9, pp. 4461–4465, Sep. 2014.

[8] D. N. Zmood and D. G. Holmes, "Stationary frame current regulation of PWM inverters with zero steady-state error," *IEEE Trans. Power Electron.*, vol. 18, no. 3, pp. 814–822, May 2003.

[9] K. Seifi and M. Moallem, "An adaptive PR controller for synchronizing grid-connected inverters," *IEEE Trans. Ind. Electron.*, vol. 66, no. 3, pp. 2034–2043, Mar. 2019.

[10] P. Santiprapan, K. Areerak, and K. Areerak, "An adaptive gain of proportional-resonant controller for an active power filter," *IEEE Trans. Power Electron.*, vol. 39, no. 1, pp. 1433–1446, Jan. 2024.

[11] Jpn. Electric Assoc., "Grid-interconnection code," JEAC 9701–2024, 2024.

[12] C. Zhai et al., "Enhanced ADRC with an improved extended state observer considering aperiodic and periodic disturbances for PMSM drives," *IEEE Trans. Ind. Electron.*, early access, doi: 10.1109/TIE.2025.3618888.